Parameter Estimation and Validation of Cascaded DC-DC Boost Converters for Renewable Energy Systems Using the IGWO Optimization Algorithm

Seyit Alperen Celtek[1*], Seda Kul[2], Selami Balci[2], Abdullah Dik[3, 4]

salperenceltek@kmu.edu.tr, sedakul@kmu.edu.tr, sbalci@kmu.edu.tr, a.dik@derby.ac.uk

[1]Department of Energy Systems Engineering, Faculty of Engineering, Karamanoglu Mehmetbey University, Karaman, Türkiye

[2]Department of Electrical and Electronics Engineering, Faculty of Engineering, Karamanoglu Mehmetbey University, Karaman, Türkiye

[3]School of Engineering, University of Derby, DE22 3AW, United Kingdom

[4]Faculty of Engineering, Iskenderun Technical University, Hatay/Iskenderun, Türkiye

Abstract: The voltage amplitude generated by renewable energy sources is often unstable, necessitating the use of power electronic circuits for effective grid integration. Among these, DC-DC converters play a critical role in maintaining a constant DC link voltage, typically 400 V or 800 V, at the input of inverter circuits that supply power to the load or the grid. The study focuses on the voltage gain behavior of a high-gain dual cascaded DC-DC boost converter designed for (photovoltaic) PV power systems. Using ANSYS Electronics software with its parametric solver, a comprehensive dataset was generated based on key parameters such as input voltage, power switch duty ratio, and switching frequency.

The Improved Grey Wolf Optimizer (IGWO) algorithm was employed to estimate mathematical models for this dataset using linear and quadratic equations. The accuracy of the proposed models was validated across six test scenarios, demonstrating superior performance compared to traditional optimization algorithms, including Harmony Search (HS), Particle Swarm Optimization (PSO), Differential Evolution (DE), and the standard Grey Wolf Optimizer (GWO). Experimental validations yielded output voltages of 23.5 V and 36.1 V for input voltages of 4.8 V and 6.2 V, respectively, closely aligning with simulation results of 23.113 V and 36.447 V.

The findings, supported by detailed simulations and graphical analyses, highlight the IGWO algorithm's precision and reliability in predicting converter output voltages under variable input conditions. This work advances renewable energy systems integration by enhancing the modeling and performance of cascaded DC-DC boost converters.

Keywords: Power electronics, Cascaded DC-DC boost converter, Parameter estimation, Renewable energy, Improved Grey Wolf Optimizer (IGWO).

1. Introduction

Renewable energy sources (RESs) are increasingly being recognized as environmentally friendly and sustainable solutions for energy generation[1]. Solar, wind, and hydroelectric power are among the most prominent sources driving this transition. However, the widespread adoption of direct current (DC) power sources in photovoltaic (PV) cells, fuel cells, and various energy storage systems has drawn significant attention to DC microgrids[2], [3]. Research into energy management and integrating renewable energy systems is vital for advancing sustainable energy technologies [4].

DC-DC converters are indispensable components in renewable energy systems, playing a critical role in converting the DC power generated by sources such as solar panels and wind turbines into alternating current (AC) for residential and commercial applications[5], as illustrated in Figure 1. These converters also regulate voltage and frequency to ensure power stability and reliability. Additionally, they facilitate energy storage in batteries or other devices, which enhances the efficiency and dependability of renewable energy systems. Consequently, Power electronics are essential for optimizing energy conversion and management in energy systems[6].

Among various DC-DC converter configurations, cascaded boost converters are particularly valued in renewable energy systems for their high efficiency, power density, voltage gain, and simple control features. Beyond voltage boosting, these converters provide critical isolation between input and output, ensuring the safety and protection of connected devices. This makes cascaded boost converters pivotal for efficiently converting low-voltage renewable energy sources into higher voltages suitable for practical applications [7].

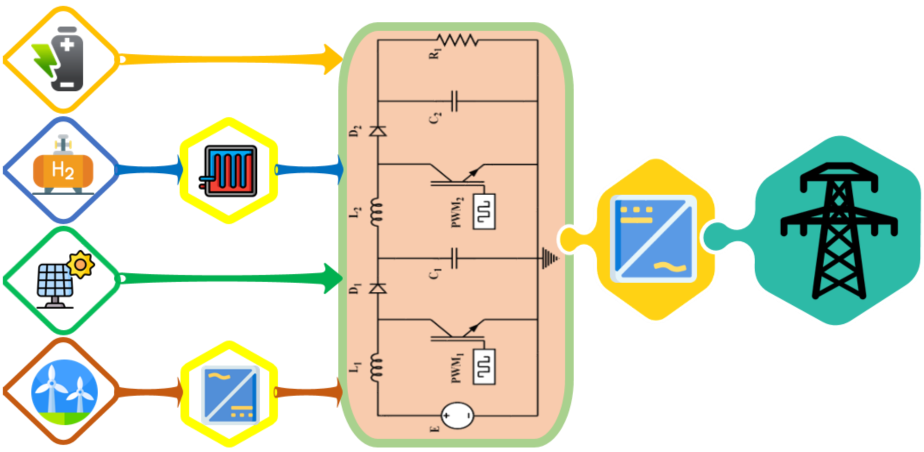

Figure 1. Renewable energy - DC/DC converter circuits systems integration

Parameter estimation is a cornerstone in the design and operation of non-linear systems, such as renewable energy systems, as it ensures accurate results and system validation. This critical process has been widely studied in the literature, with methods ranging from artificial neural networks (ANNs) and machine learning (ML) to optimization algorithms. Some notable examples include:

- Marine Predator Algorithm for PV cell models: In [8], the Marine Predator Algorithm was applied to estimate the parameters of a double-diode PV cell model. The study reported a sum of individual absolute errors for the output current and power as 0.02133487 A and 0.00876895 W, respectively. When compared to RTC France data, the root mean squared error (RMSE) was calculated as 9.8388×10^{-4}A, demonstrating the algorithm's accuracy.
- ANN-based PV power estimation: A study in [9]applied an ANN model to estimate PV power output in a photovoltaic facility in southern Italy. Weather scenarios were used to create a comprehensive dataset for training and testing the ANN model. The ANN successfully predicted PV power output with a normalized root mean squared error (nRMSE) of less than 10% across all weather conditions, demonstrating its reliability and effectiveness.
- Comparison of Traditional Estimation Methods: In[10], estimation methods, including Proportional-Integral-Derivative (PID), Artificial Intelligence (AI), Genetic Algorithm (GA), and Fuzzy Logic (FL), were comprehensively evaluated for their effectiveness in predicting PV system performance and solar radiation. The study highlighted the varying successes of these methods in practical application to PV systems.
- Review of AI-based approaches: A review in [11] examined the advantages of AI-based methodologies, such as ANN, FL, GA, Evolutionary Strategies (ES), and Harmony Search (HS), in addressing key challenges in renewable energy systems. These challenges include forecasting and modelling meteorological data, simulation, control, and system sizing for PV systems, highlighting the versatility of AI-based methods.
- Particle Swarm Optimization (PSO) for energy management: Another application in [12] employed the PSO algorithm to estimate parameters for the energy management system. The method achieved significant error reduction of 59% and 56% compared to experimental data, with an RMSE of 0.1245. The study also reported a strong correlation coefficient (R = 0.9927) between predicted and experimental results, emphasizing the robustness of the PSO approach.

Parameter estimation is also a fundamental aspect of DC-DC converter design, particularly in renewable energy systems, where it plays a critical role in ensuring efficient and reliable operation. There is an increasing interest in using optimization algorithms and artificial neural networks in parameter estimation processes in power electronic circuits used in renewable energy sources [13], [14]. For instance, AI-based estimators have been successfully utilized to predict the performance of DC-DC converter models using machine-learning techniques. These estimators have demonstrated their ability to accurately predict the performance of commercially available converters by analyzing parameters such as output voltage, input voltage, and output current [15]. Another notable study [16] proposed an artificial neural network (ANN)-based control method to manage active and reactive power in a single-phase grid-connected fuel cell system. It utilizes a DC-DC boost converter to regulate the voltage level produced by PEM fuel cells, ensuring stability through control methods that maintain the output voltage at a reference level. In this work [17], the ANN model was hybridized with the PSO algorithm to optimize syngas production in a biomass gasification plant and predict biomass requirements to meet energy demand, achieving significant improvements in energy conversion efficiency.

Despite advancements, inaccuracies in parameter estimation can result in significant drawbacks, such as voltage regulation errors, reduced efficiency, or damage to the converter or connected systems[18], [19]. Such issues highlight the need for robust and reliable estimation techniques to ensure the proper functioning of DC-DC converters in real-world applications. Despite advancements, several challenges persist in implementing parameter estimation and reliability prediction techniques for DC-DC converters. These challenges include limited data availability, complex failure modes, environmental variability, and cost considerations. However, addressing these obstacles is crucial for developing accurate models and designing robust systems that ensure efficiency and reliability over the lifetime of these converters. Accurate parameter estimation thus remains vital for optimizing renewable energy systems.

For instance, long short-term memory (LSTM) networks have been applied in maximum power point tracking (MPPT) systems to estimate battery state of charge (SOC) and current energy production[20]. The estimation process achieved mean absolute error (MAE) values between 0.0177 and 0.0431, and RMSE values between 0.0221 and 0.0790, showcasing the potential of such approaches. Additionally, parametric analyses in [21] demonstrated the effectiveness of artificial hybrid estimation intelligence techniques for achieving stable output voltage in DC-

DC converters under varying conditions, including different switching frequencies, input voltages, and duty ratio values.

The limitations of traditional methods, including slow convergence, the risk of getting stuck in suboptimal solutions, and high computational costs, necessitate exploring advanced approaches Metaheuristic methods, such as the Improved Grey Wolf Optimizer (IGWO), address these limitations by enabling faster convergence, effective parameter exploration, and reduced computational requirements [22], [23]. Despite the extensive simulation-based studies in the literature, experimental validation under real-world conditions is still limited, particularly for high-gain, dual-stage DC-DC converters.

The intermittent nature of renewable energy generation and the challenges of efficiently managing and converting power necessitate the optimization of DC-DC boost converters for higher voltage gain and energy efficiency. This work aims to address these challenges by applying advanced optimization techniques to improve the performance of a dual-stage DC-DC boost converter used in photovoltaic systems. By developing an advanced parameter estimation methodology, this study contributes to more reliable and efficient energy conversion systems.

The paper makes the following contributions:

- Proposes a novel methodology for parameter estimation of cascade boost DC-DC converters in PV systems using a metaheuristic-based modeling approach.
- Investigates the relationship between the input voltage, duty ratio, output voltage, and switching frequency in cascade boost converters, a topic that has been minimally explored in existing studies.
- Optimizes parameters to minimize output voltage fluctuation, improving system stability and efficiency.
- Demonstrates the use of GWO and IGWO for parameter estimation in cascaded boost converters, providing experimental validation through real-world tests.

The findings presented in this paper highlight the effectiveness of IGWO in addressing parameter estimation challenges and advancing the integration of renewable energy systems by improving the efficiency and reliability of power electronics circuits.

Figures 2 and 3 visually summarize the workflow and methodology of the study. Figure 2 provides a detailed representation of the process, starting with parameter acquisition through parametric analysis using ANSYS. Key inputs such as duty cycle, input voltage, and switching frequency are highlighted. The process continues with optimization using IGWO, GWO, PSO, and DE algorithms, followed by validation of the computed results. Finally, the validated parameters are tested and compared to assess the performance and accuracy of the proposed approach. Figure 3 complements this by outlining the step-by-step methodology. The workflow begins with parametric analysis in ANSYS to obtain the necessary data (Step 1 and Step 2). The data is then applied in the optimization procedure (Step 3), using both linear and quadratic modeling techniques. The optimized results are validated (Step 4) and compared against experimental results (Step 5) to evaluate the effectiveness of the proposed methodology.

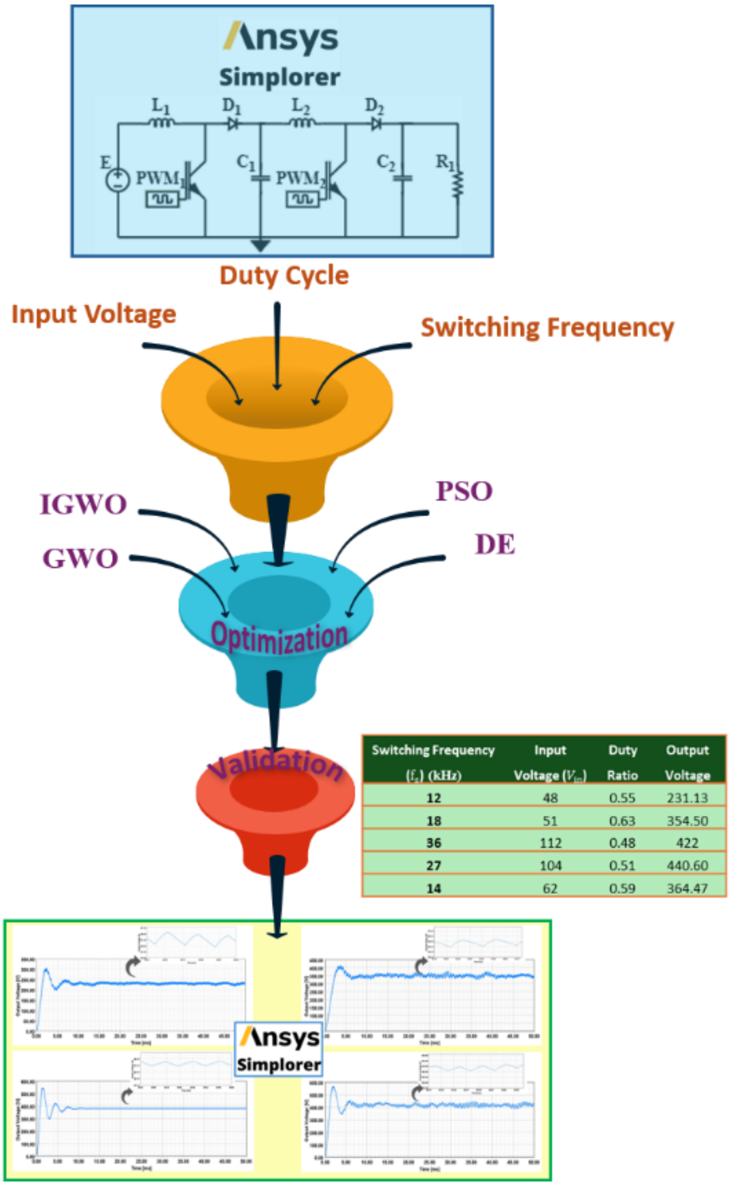

Figure 2. Visual workflow of the study

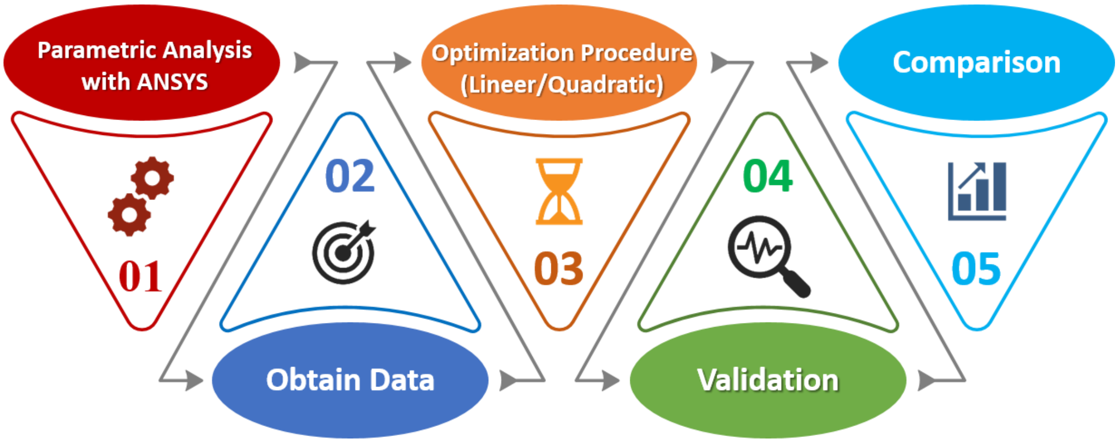

Figure 3. Methodology framework of the study (template by PresentationGO [24])

2. System Design and Parameter Estimation Framework

This section describes the high-gain DC-DC boost converter utilized in this study, highlighting parametric simulation studies and the data set preparation techniques. Additionally, the IGWO algorithm, one of the advanced parameter estimation methods, is discussed in detail.

2.1. DC-DC Boost Converter Systems

High-gain DC-DC power converter circuits are widely used in power systems such as PV systems where voltage stability is a critical issue. The use of a conventional boost converter in these systems is not a practical technique because it will cause significant losses and low efficiency when the upper voltage range cannot be created and the duty cycle of the switch is high. To eliminate this problem, topologies such as cascade boost converter and quadratic boost converter are preferred. Moreover, they provide higher voltage gain without the need for high duty-cycle like conventional, but they have some problems such as lower efficiency and higher losses [25].

In this study, cascade boost converter topology is used due to its simple structure, easy maintenance, and high flexibility features. The dual-stage boost converter, shown in Figure 4, is designed by combining two equivalent base amplifiers connected in tandem. It consists of an input voltage source (V_{in}), two independently controllable semiconductor switches, two free diodes (D_1 and D_2), two capacitors (C_1 and C_2), and two inductors (L_1 and L_2) [26].

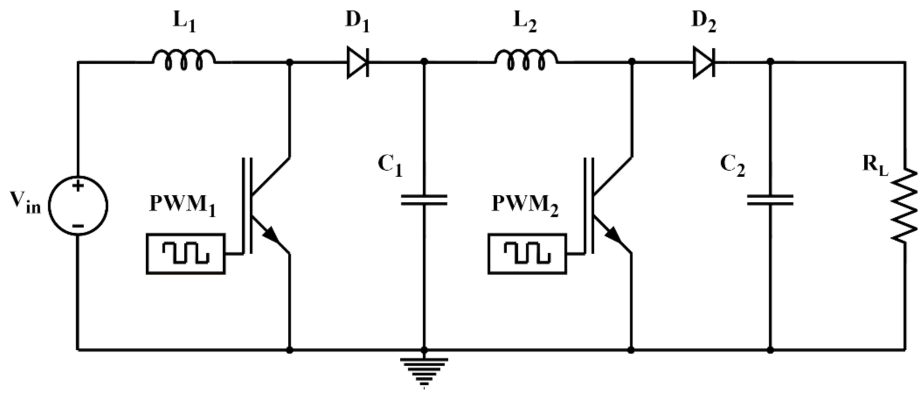

Figure 4. Double cascaded DC-DCboost converter circuit [26]

Operating Mode 1: In this state, switch $Q_1$is turned on, while Q_2 remains off. The inductorL_1 is charged with the supply voltage and stores energy. This mode ends when Q_1 is turned off. The operation of this mode is illustrated in Figure 5.

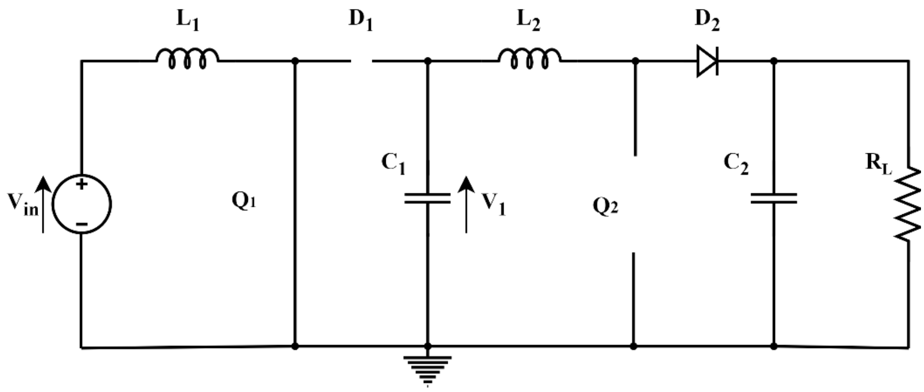

Figure 5. Mode 1 condition of double cascaded boost converter[26]

Operation Mode 2: During this period, Q_1 is off, and Q_2 is turned on, as shown in Figure 6. The output of the first stage (V_1) becomes the input for the second stage. Inductor L_2 is charged with the supply voltage and stores energy. This step concludes when S_2 is turned off. The converter operates in continuous conduction mode across these two stages.

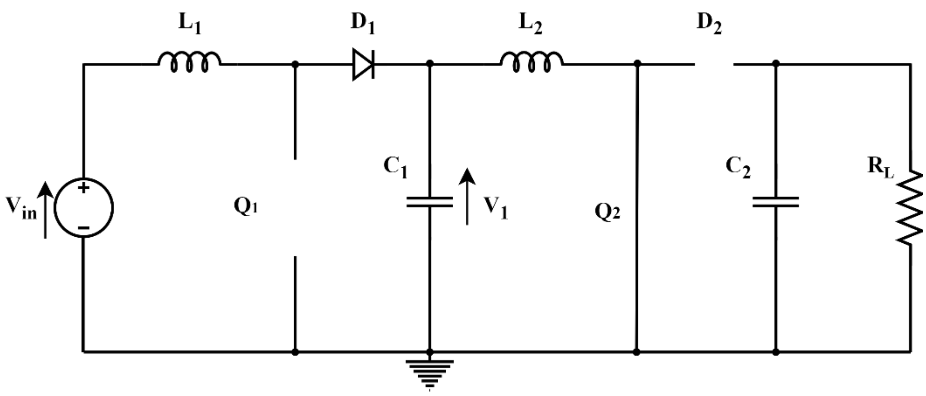

Figure 6. Mode 2 condition of double cascaded boost converter[26]

The output voltage (V_0) of the step-up converter is derived using the first-stage boost voltage (V_{c1}), and the second-stage boost voltage (V_{c2}), as given by Eqs. (1)-(3) [27], [28]. It is emphasized that the duty cycles of the two switches in the cascaded boost converter circuits are the same in Eq. (3) and the gain value is multiplied. Thus, both power switches operate at the same duty ratio. For this circuit topology, the duty ratios are accepted as $D_1 = D_2 = D$. Thus, a quadratic gain proportional to the square of the gain of a boost circuit can be achieved.

$$\frac{V_{c1}}{V_{in}} = \frac{1}{1-D} \tag{1}$$

$$\frac{V_{c2}}{V_{c1}} = \frac{V_0}{V_{c1}} = \frac{1}{1-D} \tag{2}$$

$$\frac{V_0}{V_{in}} = \frac{1}{(1-D)^2} \tag{3}$$

To achieve the desired gain value (K_{gain}), Eq. (4) is used to calculate the duty ratio (D)of the switching elements.

$$D = 1 - \frac{1}{\sqrt{K_{gain}}} \tag{4}$$

However, the theoretically calculated gain value and switching element duty factor are practically limited to 0.65 to prevent the power switch from being subjected to stress during high-frequency turn-on and turn-off transitions. Therefore, it is recommended not to exceed the value of 0.65 in practice [27], [28]. The relationship between K_{gain} and D is depicted in Figure 7.

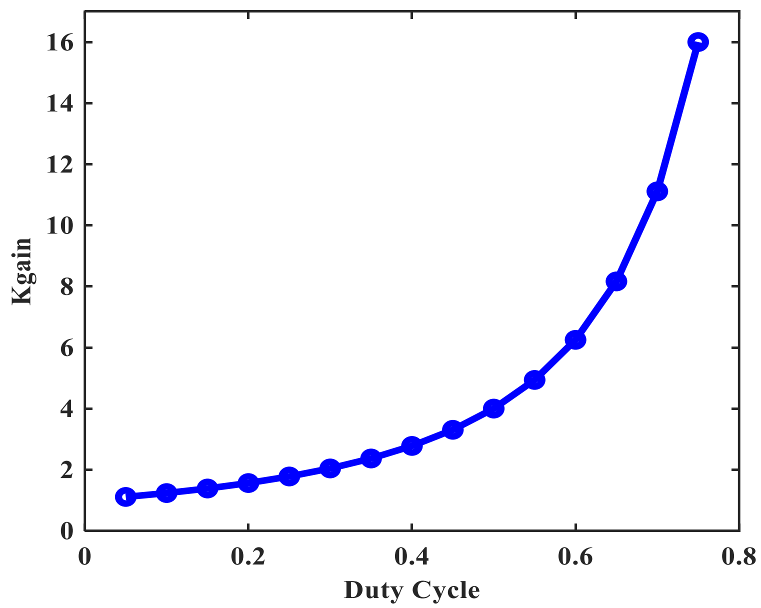

Figure 7. K_{gain}-D relationship according to switching parameters.

2.2. IGWO Algorithm

The IGWO algorithm is an advanced optimization method inspired by the natural hunting behavior of wolves. Its primary objective is to identify parameters that yield the optimal value of a given function. IGWO enhances the standard GWO algorithm [29] by addressing limitations such as population diversity, the imbalance between exploration and exploitation, and early convergence [30], [31].

IGWO employs a dynamic strategy where leader wolves are selected randomly from the top three wolves in each iteration, ensuring better search space exploration. The algorithm models wolf hunting behavior more effectively by incorporating a specific distribution and increasing the number of aggressive wolves, leading to faster convergence.

The IGWO algorithm consists of three main phases: initialization, movement, and selection/update phases.

<u>Initialization Phase:</u> The IGWO algorithm defines a range to determine the possible solution area. The initial positions of the individuals are chosen randomly within this range. Initially, wolves (N: number of wolves) are randomly distributed in the search space in the list of [l_j, u_j].The initial positions (X_{ij}) are determined as follows:

$$X_{ij} = I_j + rand_j\,[0,1]\,x\,(u_j - l_j),\ \ i \in [1, N], \qquad j \in [1, D] \tag{5}$$

Where $X_i(t) = \{X_{i1}, X_{i2}, \ldots. X_{iD}\}$ represents the i^{th} position in the t^{th} iteration (D=dimension). The population is recorded in a matrix with N rows and D columns.

<u>Movement Phase:</u> In this phase, The IGWO computes the next position of the wolf $X_i(t)$. For this computation, IGWO uses the wolf's different neighbors and a randomly selected wolf from the matrix. The $R_i(t)$ is indicates the radius between the current position $X_j(t)$ and the position of the candidate $X_{j-GWO}(t+1)$is given by:

$$R_i(t) = \left|X_j(t) - X_{j-GWO}(t+1)\right| \tag{6}$$

The neighbors($N_i(t)$)are calculatedusing:

$$N_i(t) = \left\{ X_j(t) \middle| D_i(X_j(t), X_j(t)) \leq R_i(t),\ X_j(t) \in Matrix \right\} \tag{7}$$

Where D_i is the Euclidean distance between$X_j(t)$ and $X_i(t)$.

Selection/Update Phase: The new position($X_{i_{DLH},d}$) for DLH model is computed as:

$$X_{i_{DLH},d}(t+1) = (X_{i,d}(t) + rand[0,1]\, x\, (X_{n,d}(t) - X_{r,d}(t)) \quad (8)$$

Where(n) is the number of wolves, and (d) is the dimension. The updated position ($X_i(t+1)$) is chosen based on the fitness value:

$$X_i(t+1) = \begin{cases} X_{i\_GWO}(t+1), & if\ f\left(X_{i\_GWO}(t+1)\right) < f(X_{i_{DLH}}(t+1)) \\ & X_{i_{DLH}}(t+1)\text{otherwise} \end{cases} \quad (9)$$

The IGWO algorithm achieves faster convergence compared to standard optimization methods and has demonstrated success in various real-world applications. By incorporating advanced hunting strategies and leader selection, IGWO ensures a balance between exploration and exploitation, making it a robust choice for parameter estimation in non-linear systems. For more detailed information about the algorithm, please refer to the study titled [30], [32].

3. Optimization Procedure for Cascaded Boost DC-DC Converter Parameter Estimation

3.1. Optimization Model Development

This section outlines the optimization procedure for cascaded boost DC-DC converter parameter estimation. A comprehensive dataset was generated using parametric simulation in ANSYS-Electronics software, as shown in Figure 8. The data set consists of 714 scenarios, with each capturing unique combinations of input voltage, duty ratio, and switching frequency. The parameter limits are summarized in Table 1, and technical specifications of the converter are provided in Table 2.

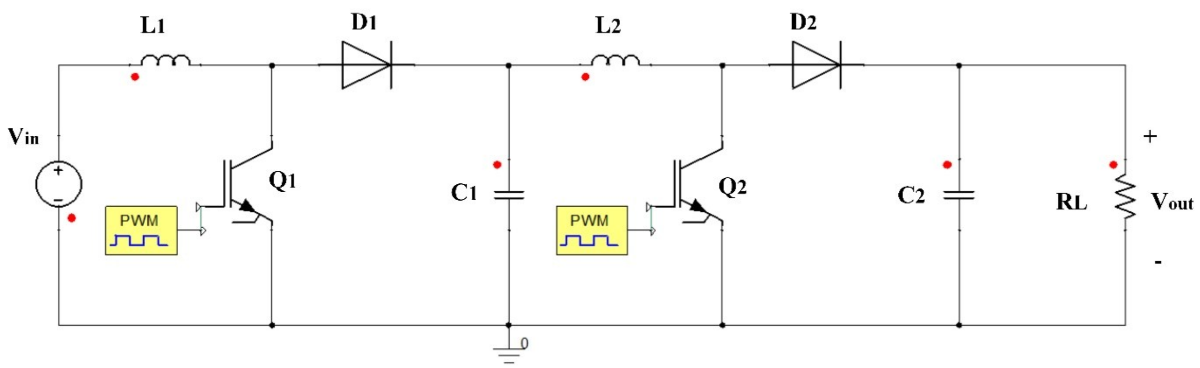

Figure 8. Parametric simulation circuit [21].

Table 1. The limit of parameters.

Parameter Name	Minimum Limit	Maximum Limit
Input Voltage	40 V	120 V

Duty Ratio	0.15	0.65
Switching Frequency	10 kHz	40 kHz

Table 2. Technical parameters of the double cascaded boost converter

Input Voltage (V_i)	40 V
Output Voltage (V_0)	400 V
First Stage Inductor (L_1)	100 μH
Second Stage Inductor (L_2)	100 μH
First Stage Capacitor (C_1)	680 μF
Second Stage Capacitor (C)	680 μF
Load	100 Ohms

In this study, the internal resistances of passive circuit elements, such as inductors and capacitors of the converter circuit, and the voltage drops of diodes and power switching elements are also neglected. Thus, parametric simulation studies are carried out under ideal conditions. The primary objective of this study is to model the parameters of the step-up DC-DC converter by analyzing the relationship between the input voltage, duty ratio, switching frequency, and output voltage. This is because, as seen in Eqs. (1)-(2), the output voltage is directly related to the duty cycle and input voltage under ideal conditions. In addition, the ripple in the output voltage varies directly and inversely proportional to the switching frequency. There is no other parameter that directly affects the output voltage under ideal conditions. An IGWO-based heuristic algorithm was employed to examine the dataset and derive mathematical relationships, expressed in linear and quadratic equations.

The linear function represents a straight-line relationship that best captures the linear correlation between the input variables and output data. The mathematical representation of this three-variable linear function is provided in Eq. (10).

$$E_{\text{linear}} = a_1 + a_2X_1 + a_3X_2 + a_4X_3 \quad (10)$$

For datasets with non-linear relationships, a linear function may fail to represent the underlying patterns in the data accurately. In such cases, more sophisticated mathematical techniques are essential. To address this, the study also models the parameter estimation for the cascade boost

DC-DC converter using a quadratic equation. The quadratic equation, which accounts for both interaction and non-linear effects among the variables, is expressed in Eq. (11).

$$E_{\text{quadratic}} = a_1 + a_2X_1 + a_3X_2 + a_4X_3 + a_5X_1X_2 + a_6X_1X_3 + a_7X_2X_3 + a_8x_1^2 + a_9x_2^2 + a_{10}x_3^2 \qquad (11)$$

The variables X_1,X_2, X_3 in Eqs. (10)-(11) represent the input voltage, duty ratio, and switching frequency, respectively. These equations aim to mathematically express the relationship between the experimental parameters listed in Table 1 and the output voltage. In these equations, $a_1$is the independent weight (constant term), while the coefficients$(a_2, a_{3,\dots}, a_{10})$are dependent weights.

The objective function, by minimizing the difference between the actual output voltage and the computed output voltage derived from Eqs. (10)–(11).

$$Objective\ Function = \sum_{n=1}^{X} (OutputVoltage_{\text{n}} - ComputedOutputVoltage_{\text{n}})^2 \qquad (12)$$

Where the X is used to symbolize the number of scenarios. The $OutputVoltage_{\text{n}}$ represents the Output Voltage value in n[th] scenario while $ComputedOutputVoltage_{\text{n}}$represents the linear or quadratic equation results obtained by Eqs. (10)-(11).

The circuit parameters derived from the output voltage model are instrumental in designing an adaptive voltage controller as seen in Figure 9. Specifically, the proposed model facilitates dynamic adjustments to the duty cycle in response to input voltage variations under different load conditions. For instance, when the converter input voltage fluctuates between 40 V and 120 V, the duty cycle of the controller adaptively adjusts within the range of 0.15 to 0.65. This ensures that the converter output voltage remains stable at 400 V, regardless of input voltage changes.

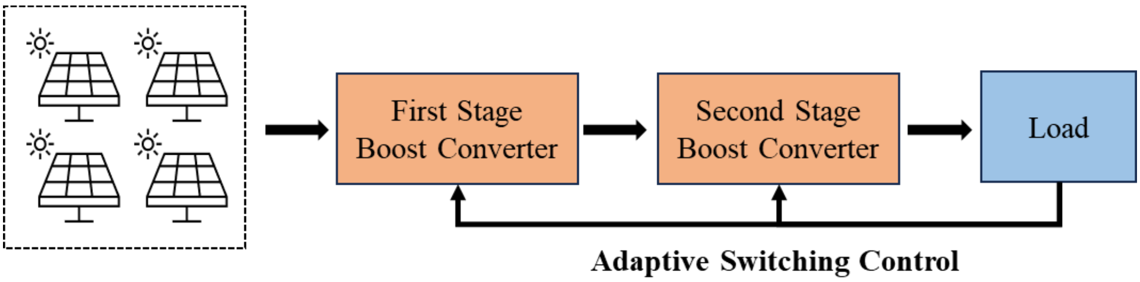

Figure 9. Block diagram of the proposed model.

The derived mathematical model provides precise guidelines for determining the optimal duty cycle based on real-time input voltage variations. These parameters can directly inform the design of a controller, ensuring robust performance and adaptability in varying operational conditions [33] [34].

4. Results for Cascaded Boost DC-DC Converter Parameter Estimation and Validation

4.1. Benchmarking of the IGWO Algorithm

The IGWO algorithm, implemented on the MATLAB platform, was validated using standard benchmark functions listed in Table 3. Benchmark functions are mathematical tools used to assess the performance of the created optimization algorithm by testing it on different features. The IGWO code was tested using six benchmark functions (f_1 to f_6), where the functions (f_1 to f_4) evaluated the convergence speed of the IGWO, and functions (f_5 and f_6)assessed exploration performance.

Table 3. The benchmark functions.

No	Function	Name
f1	$\sum_{j=1}^{m} y_j^{2}$	Sphere
f2	$\sum_{j=1}^{m} \lvert y_j \rvert + \prod_{j=1}^{m} \lvert y_j \rvert$	Schwefel 2.22
f3	$\sum_{j=1}^{m} \left(\sum_{i=1}^{j} y_i \right)^{2}$	Schwefel 1.2
f4	$\max_j \{ \lvert y_j \rvert, 1 \leq j \leq m \}$	Schwefel 2.21
f5	$\sum_{j=1}^{m} \left[y_j^{2} - 10\cos(2\pi y_j) + 10 \right]$	Rastrigin
f6	$-20\exp\left(-0.2 \left(\frac{1}{m} \sum_{j=1}^{m} y_j^{2} \right)^{\wedge} 0.5 \right) - \exp\left(\frac{1}{m} \sum_{j=1}^{m} \mathrm{Cos}(2\pi y_j) \right) + 20 + e$	Ackley

IGWO was run 25 times for each function to ensure statistical reliability. The results, including the mean value and standard deviation (SD), are shown in Table 4. A lower SD indicates better consistency in the algorithm's performance.

Table 4. Results of benchmark test functions

Methods		f1	f2	f3	f4	f5	f6
IGWO	MEAN	2.31E-195	4.74E-206	0	2.91E-209	0	8.88E-17
	SD	0	0	0	0	0	0

4.2. Results for Cascaded Boost DC-DC Converter Parameter Estimation

The IGWO-based optimization model was applied to parameter estimation for the cascaded boost DC-DC converter. The weights in Eqs. (10)–(11) were optimized over 25 runs. The average of the best results yielded the following linear and quadratic equations:

$$E_{\text{linear}} = -98 - 1{,}3569\, X_1 + \; 1{,}6878 X_2 + 6{,}3416 X_3 \tag{13}$$

$$E_{\text{quadratic}} = -0{,}2771 - 0{,}14\, X_1 + \; 3{,}6193 X_2 - 11.5229\, X_3 - 0{,}0144 X_1 X_2 + \; 1{,}9259E5\, X_1 X_3 \\ + \; 0{,}0807 X_2 X_3 \pm \; 0{,}0280\, x_1^2 - \; 0{,}0191 x_2^2 + \; 0{,}1747 x_3^2 \tag{14}$$

The best optimization scores obtained using Eq.(12) are 46,5629 for the linear model and 0,1314 for the quadratic models. Figures 10 and 11 demonstrate the convergence trends of the IGWO and Classical GWO methods for parameter estimation. In these figures, the objective function, as defined in Eq. (12), represents the difference between computed and measured values. Figure 10 represents the convergence trend for the linear model, while Figure 11 depicts the quadratic model. In both cases, the objective function value falls below 10 within 100 iterations, demonstrating the rapid convergence of the IGWO method. Compared to classical GWO, IGWO achieves faster convergence, as evidenced in both figures. These results confirm IGWO's superior performance and its high convergence speed in solving the cascaded boost DC-DC converter parameter estimation problem.

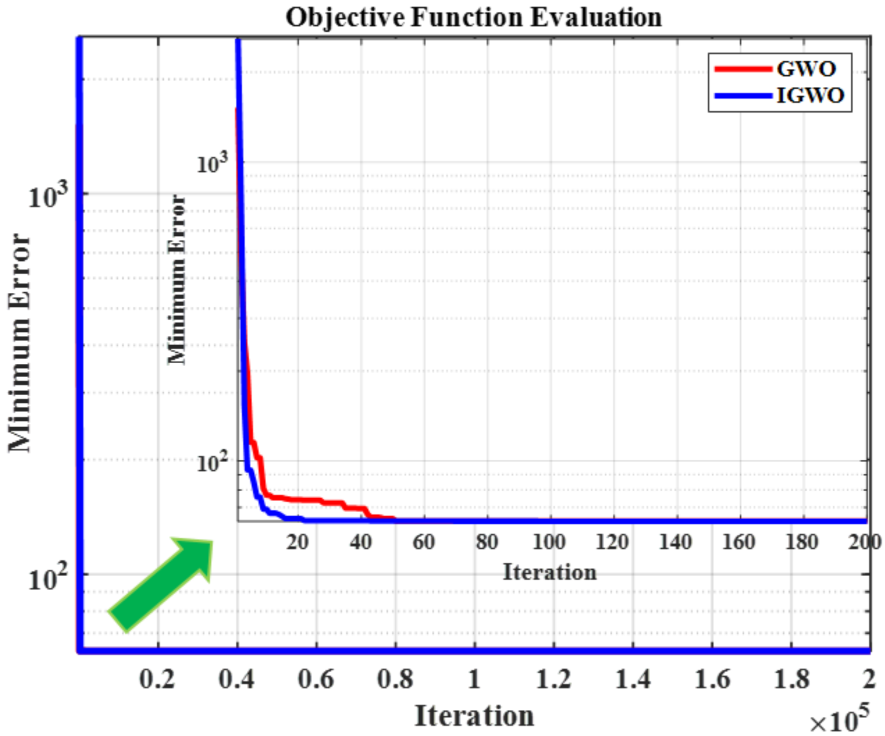

Figure 10. Convergence of IGWO and GWO for the linear model

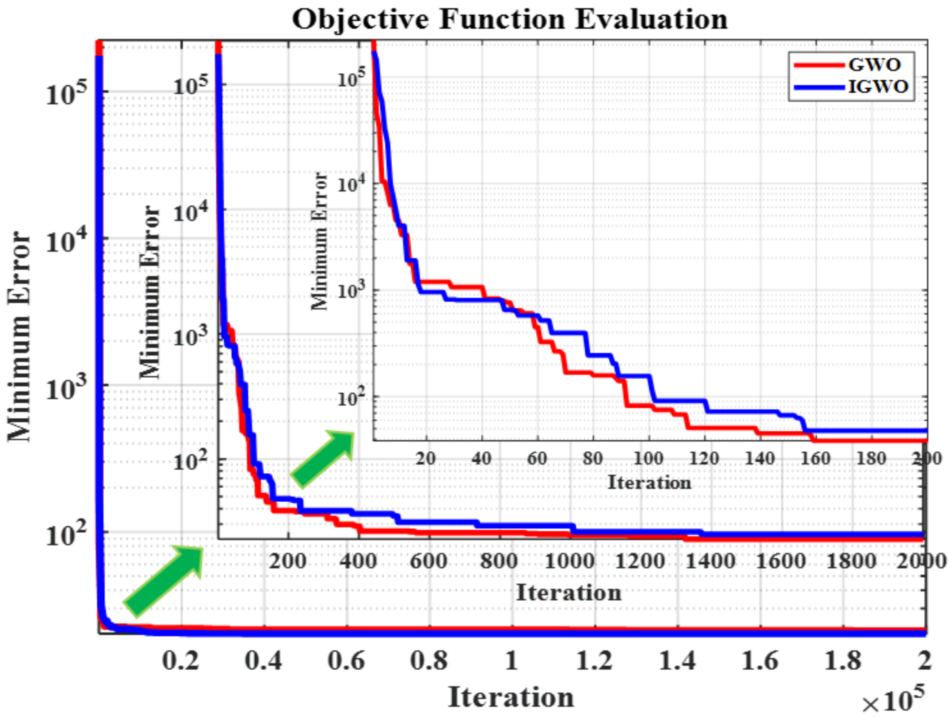

Figure 11. Convergence of IGWO and GWO for the quadratic model

This paper evaluates the accuracy of the heuristic-based IGWO method through four key approaches: validation using an independent data set, comparative analysis, performance metrics, and comparison with actual data. An independent validation data set distinct from the original data set was employed to assess the accuracy of the proposed prediction method. IGWO's prediction results have been compared with other commonly used classical optimization methods, such as PSO, DE, and GWO. Various performance measures (Mean Absolute Error, Mean Absolute Percentage Error, Mean Squared Error, and Sum of Squared Errors) are used to evaluate the IGWO-based prediction model's performance. Additionally, IGWO's estimation results were validated against actual data obtained using the ANSYS Twin Builder simulation program, which enables observation of the prediction model's performance under real-world conditions. This comprehensive evaluation demonstrates the robustness and reliability of the IGWO method in accurately modeling the cascaded boost DC-DC converter parameters.

4.3. Validation and Comparison

This section explains the validation experiments for the estimation model used for the cascaded boost DC-DC converter parameter estimation. Table 5 shows the validation data for five scenarios used in this work. These five scenario points, completely independent of 714 scenarios, were selected to evaluate the performance of this function. The validation dataset consists of new samples located outside of the original dataset. These selected data were used to test the function's generalizability.

Table 5. Validation dataset

Switching Frequency (f_s) kHz	**Input Voltage (V_{in}) V**	**Duty Ratio**	**Output Voltage V**
12	48	0.55	231.13
18	51	0.63	354.50
36	112	0.48	422
27	104	0.51	440.60
12	48	0.55	231.13

The actual output voltage values of the validation dataset selected for performance evaluation were compared with the values predicted by the function. The performance of the linear and quadratic models was evaluated using error metrics: MAE, MAPE, MSE, and SSE, as listed in Table 6.

Table 6. Performance evaluation results

Methods	**MAE**	**MAPE**	**MSE**	**SSE**
Linear	46.59	13.8609	3.2E3	1.97E4

Quadratic	0.1314	0.0355	0.0660	0.3962

MAE represents the mean value of the absolute differences between predicted and actual values. It considers the balance between positive and negative errors and is expressed in units. A lower MAE value indicates that the estimate is closer to the actual value. The MAE results of linear and quadratic models are 46.59 and 0.1314, respectively.

MAPE shows the error the predicted values make concerning the actual values in percentage terms. The absolute percentage errors are averaged for each observation. It is usually expressed as a percentage and represents the ratio of the predicted value to the actual value. The linear model's MAPE is 13.8609, while the quadratic's MAPE is 0.0355. The lower the MAPE value, the result of quadratic's MAPE, the closer the estimate is to the true value.

MSE is the mean of the squares of the differences between predicted and actual values. Positive errors carry more weight and are expressed in units. The result of the quadratic model is 0.0660. A smaller MSE value indicates the estimate is closer to the actual value.

SSE refers to the sum of the squares of the differences between predicted and actual values. The computed SSE values are 1.97E4 and 0.3962 for linear and quadratic models, respectively. A lower SSE indicates that the estimate is closer to the exact values.

The results, shown in Table 6, indicate that the quadratic model outperforms the linear model in all metrics. As a result of this comparison, it has been measured that the values calculated by the quadratic function are close to the actual values.

Table 7 compares the cases where quadratic function results were obtained using classical optimization methods such as GWO, PSO (Particle Swarm Optimization), DE (Differential Evolution), HS (Harmonic Search), and GA (Genetic Algorithm). Table 7 presents each method's prediction results and the criteria used to evaluate their accuracy.

Table 7. Comparison of quadratic model with classical methods

Methods	MAE	MAPE	MSE	SSE
IGWO	0.1314	0.0355	0.0660	0.3962
GWO	0.2195	0.0577	0.0929	0.5573
PSO	3.2195	0,9425	19.1316	114.7899
DE	3.3663	0.9720	20.040	120.2399
HS	3.3797	0.9840	21.020	122.337
GA	4.0120	1.0032	24.0068	140.297

First, when the mean absolute error (MAE) values are examined, IGWO has the lowest MAE value (0.1314). These MAE results show that IGWO's estimates are closer to the actual values. The MAE value of GWO (0.2195) is slightly higher than that of IGWO, but the MAE values of PSO, DE, GA, and HS methods are significantly higher (3.2195, 3.3663, 4.0120, and 3.3797, respectively).

Secondly, considering the average absolute percentage error (MAPE) values, IGWO again has the lowest MAPE value (0.0355). This shows that IGWO's forecasts make fewer errors than the actual values. On the other hand, the MAPE values of different methods are higher than those of IGWO.

Thirdly, when the mean square error (MSE) and the sum of square error (SSE) values are examined, IGWO has the lowest MSE and SSE values. MSE results confirm that IGWO's estimates are closer to the actual values. The MSE and SSE values of GWO, PSO, DE, GA, and HS are higher, confirming the superior performance of IGWO in minimizing the error between predicted and actual values.

As demonstrated in Table 7, the IGWO method consistently outperforms other optimization techniques. Among the methods evaluated, wolf-based systems such as GWO and IGWO yield superior results compared to classical approaches. By mimicking the leadership and hunting strategies of grey wolf packs [35], these methods effectively address problem diversity and complexity.

IGWO, an enhanced version of GWO, has been recognized in the literature for its improved convergence speed [30]. It achieves faster and more accurate solutions by refining the exploration and exploitation balance, enabling better analysis of relationships between various parameters. Additional advantages of IGWO include its ability to operate within a more expansive solution space and its superior global search performance.

The findings presented in Figure 11 and Table 7 further validate IGWO's effectiveness, corroborating its reported success in the literature. These results highlight IGWO as a robust and efficient tool for addressing cascaded boost DC-DC converter parameter estimation challenges.

The Friedman test is a non-parametric test used to compare the performance of multiple algorithms. The Friedman test is commonly used to evaluate the performance of heuristic algorithms, where each algorithm is ranked according to a performance metric, and these ranks are compared statistically.

According to the Friedman ranking test results in Table 8, IGWO was ranked as the best-performing method. GWO was ranked second, while HS, DE, and PSO took third, fourth, and fifth places, respectively. The results in Table 7 show that IGWO performs better than other methods, outperforming the heuristic optimization methods. The Friedman rank test statistically evaluates these performance differences and reveals that IGWO is more successful than other methods. These results indicate that IGWO is one of the most effective methods that can be preferred for a cascaded DC-DC boost converter parameter estimation problem.

Table 8. Friedman ranking test results.

Methods	IGWO	GWO	HS	DE	PSO	GA
Friedman Rankings	1	2	3	4	5	6

Parametric simulation studies and data set analysis based on the IGWO-based method have provided valuable information about the voltage gain behaviour of the cascaded DC-DC boost converter circuit for renewable energy systems. It has been observed that the voltage gain is affected by various parameters, such as the input voltage, the duty ratio of the power switches, and the switching frequency. Thus, it became clear that optimizing these parameters can significantly improve circuit performance and efficiency. According to the parameters given in Table 2, the power electronics circuit software runs to prove the accuracy of the proposed method, and the converter output voltage graph for the input variables given in Figure 12 is shown. Accordingly, while the input variables of the parametric simulation were f_s=12 kHz, V_{in}=48 V, and duty ratio=0.55, the converter output voltage value was determined as approximately 231V.

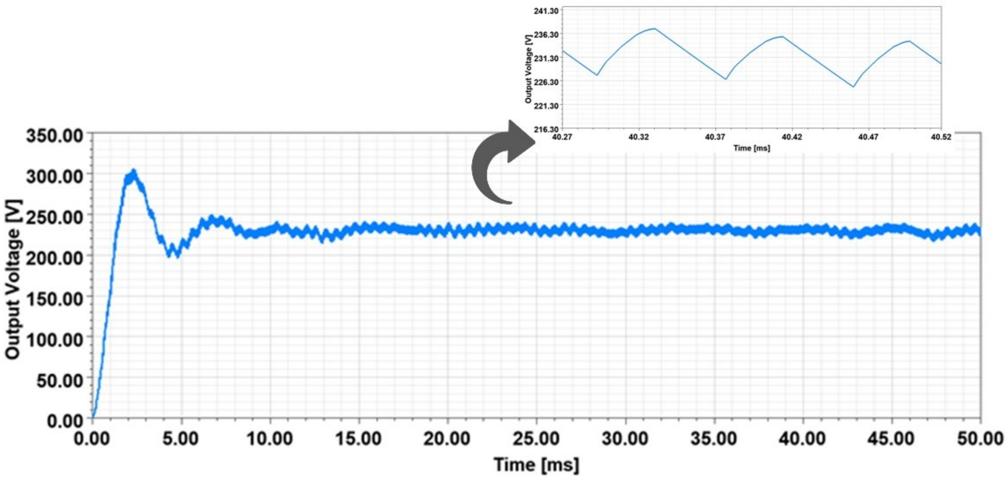

Figure 12. Output voltage waveform in f_s=12 kHz, V_{in}=48 V, duty ratio=0.55 situation.

Likewise, when the input variables of the power electronics circuit are set as fs=18 kHz, V_{in}=51 V, and duty ratio=0.63, the converter output voltage value becomes approximately 354 V, as given in Figure 13.

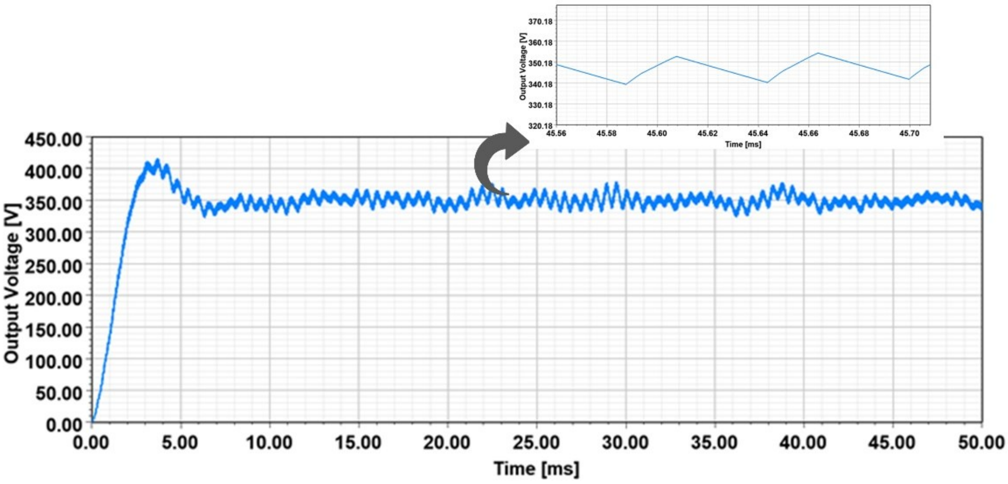

Figure 13. Output voltage in f_s=18 kHz, V_{in}=51 V, duty ratio=0,63 situation.

Since the increase in the switching frequency value reduces the converter output voltage's ripple value, the output voltage's increase is essentially adjusted with the duty ratio parameter. As seen in Figure 14, the duty ratio is reduced to 0.43 when the converter input voltage value increases.

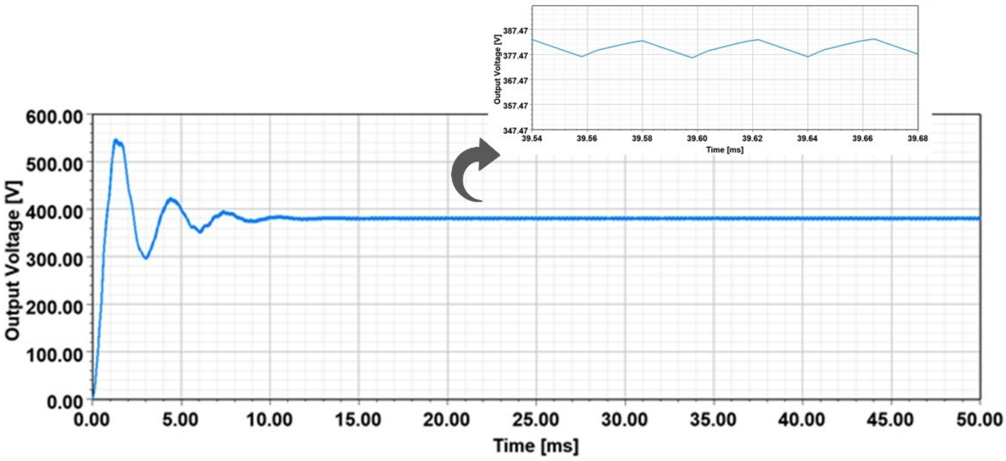

Figure 14. Output voltage in f_s=24 kHz, V_{in}=125 V, duty ratio=0,43 situation

As given in Figure 15, when f_s=27 kHz, V_{in}=104 V, and duty ratio=0.51, the converter output voltage value comes to approximately 440 V. Also, with the increased switching frequency, the ripple in DC voltage is smaller in amplitude. In grid integration circuits, DC bus voltages are usually kept constant at 400 V at the inputs of the inverters. Thus, even if the converter input voltage changes, the DC bus voltage can quickly be brought to the desired value by setting the switching variables in Figure 15.

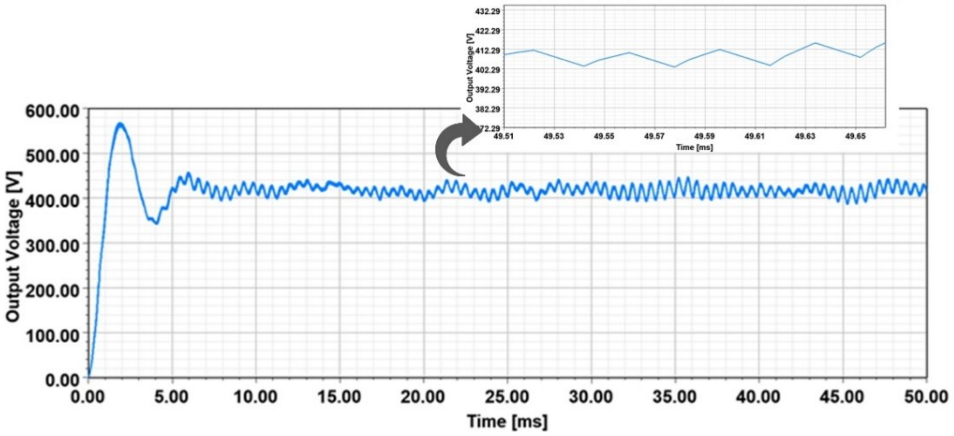

Figure 15. Output voltage inf_s=27 kHz, V_{in}=104 V, duty ratio=0,51 situation

To see the ripples in the output voltage caused by load changes, a parametric simulation was run for the proposed cascaded DC-DC boost converter in the 5-30 Ohm load range, and the output voltage levels, and ripple levels seen in Figure 16 were obtained. This simulation resulted in a difference between 340-370 V load changes on the load for the switching parameters f_s=24 kHz, V_{in}=125 V, and duty ratio = 0.43. Thus, it was seen that the output voltage was not affected much by load changes. This difference of approximately 30 V is a change that the duty ratio can compensate for.

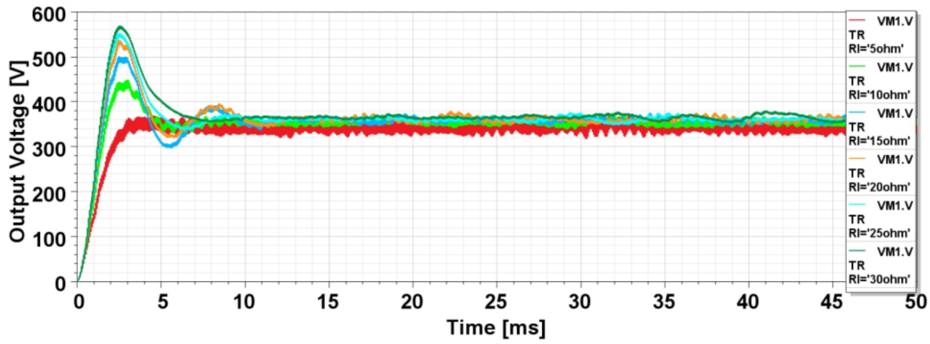

a

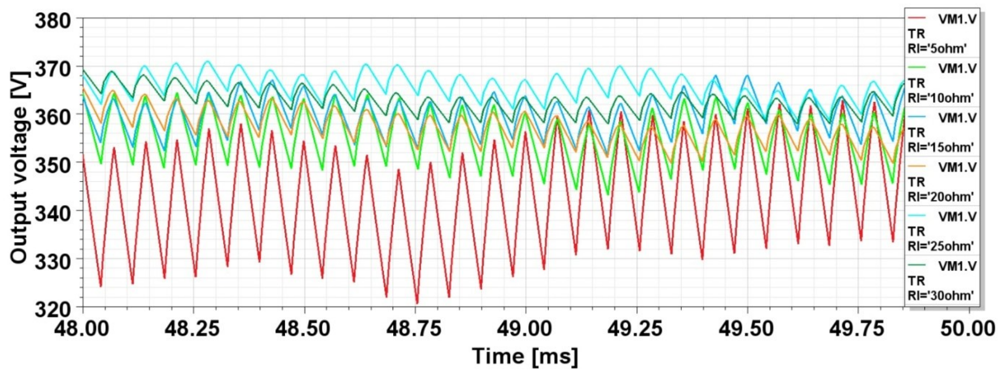

b

Figure 16. a) Parametric output voltage according to different load conditions, **b)** Voltage ripple differences in 48-50 ms.

4.4. Experimental Validation

To validate the proposed method, an experimental setup was designed to replicate the conditions outlined in the parametric dataset. The input variables were carefully controlled to match the values used for simulation, allowing for a direct comparison between the theoretical predictions and actual experimental results.

The experimental outcomes were recorded based on the parameters provided in Table 5. In two different experiments, the switching frequency, input voltage, duty ratio, and output voltage parameters were defined, and the output voltage values were measured under these conditions.

The double-cascaded boost converter-based experimental setup was designed using two DC-DC boost converters connected in series. The physical parameter values used in the double-cascaded boost converter are provided in Table 2. The input voltage values for the experiments were limited to 15 volts in the experimental setup, which is why the values in Table 5 have been scaled down by a factor of 1/10 to match the experimental conditions.

Table 9. Experimental results of the proposed method.

Switching Frequency (f_s) (kHz)	Input Voltage (V_{in}) (V)	Duty Ratio	Output Voltage (V)	Exp. Output Value (V)
12	4.8	0.55	23.113	23.5
14	6.2	0.59	36.447	36.1

Table 9 shows the experimental results of the proposed method. In the first experiment, the switching frequency was set to 12 kHz, input voltage to 4.8 V, and duty ratio to 0.55, with a theoretical output voltage of 23.113 V. The experimental measurement yielded an output voltage of 23.5 V, which is in close agreement with the theoretical value. The corresponding experimental setup for this test is shown in Figure 17 below.

Figure 17. Experimental setup for 12 kHz switching frequency, 4.8 V input voltage, and 0.55 duty ratio.

In the second experiment, the switching frequency was set to 14 kHz, the input voltage to 6.2 V, and the duty ratio to 0.59. The theoretical output voltage was calculated to be 36.447 V, while the experimental output voltage was 36.1 V. This also shows a close match with the theoretical prediction. The experimental setup for this test is shown in Figure 18.

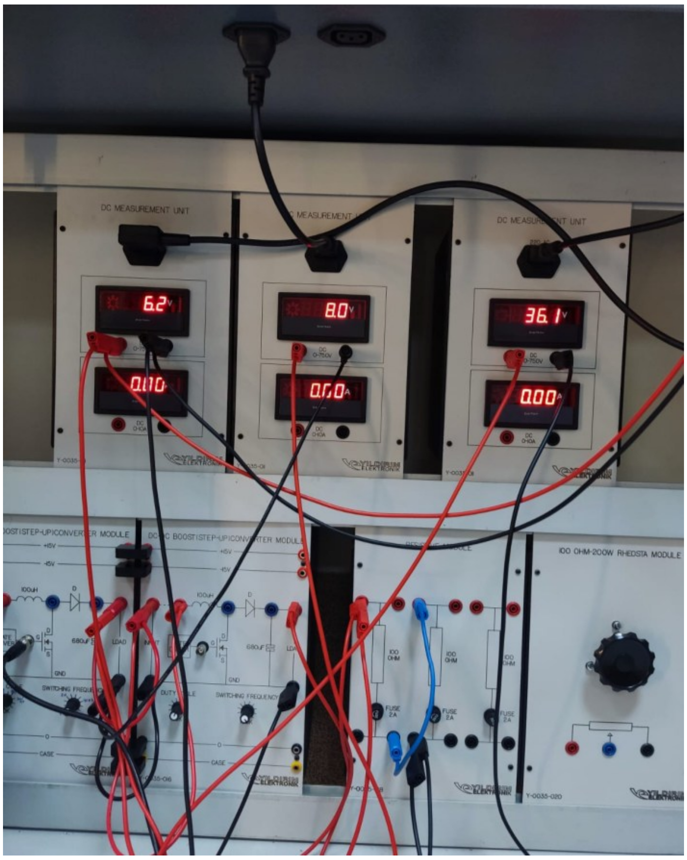

Figure 18. Experimental setup for 14 kHz switching Frequency, 6.2 V input Voltage, and 0.59 Duty Ratio.

The experimental results, when compared to the theoretical values, confirm the reliability and accuracy of the proposed method. This consistency demonstrates that the method can be effectively applied in real-world scenarios.

5. Conclusions

This study comprehensively analyses the voltage gain behaviour of step-up DC-DC amplifier circuits designed for renewable energy systems. Through parametric simulation studies and dataset analysis, the key parameters influencing voltage gain were identified, and their effects on circuit performance were investigated.

The IGWO algorithm was successfully applied to optimize the input and output variables of the amplifier circuit. The results demonstrate that IGWO effectively enhances both voltage gain and the circuit's overall efficiency. Figures 9–18 present evidence supporting these conclusions. These findings highlight IGWO's potential for designing and optimizing power electronic circuits in renewable energy systems.

The experimental validation of the proposed method showed that the output voltages from the two experiments were 23.5 V and 36.1 V for input voltages of 4.8 V and 6.2 V, respectively, which closely matched the simulation results (23.113 V and 36.447 V). These results indicate the effectiveness of the IGWO method in predicting and optimizing the performance of the circuit. The quadratic model, which exhibited better prediction accuracy than the linear model, highlighted the advantages of using IGWO for renewable energy applications.

The electrical energy obtained from solar panels produces an unstable DC voltage and is likely to change at any time during the day. Therefore, the proposed method is important in ensuring the efficiency and reliability of power electronic circuits, such as adaptive duty ratio control to keep the output voltage constant at a certain level. Thus, it can increase the efficiency and productivity of high-gain DC-DC power converter circuits that can be used in grid interfaces of renewable energy sources.

A key finding of this study is IGWO's effectiveness in estimating and optimizing the input and output variables within the dataset. The algorithm demonstrated its capability to efficiently search parameter space and converge to optimal or near-optimal solutions, making it a robust tool for designing and optimizing power electronics circuits in renewable energy systems.

The quadratic model's superior performance, as evidenced in Table 6, illustrates its ability to produce predictions closer to actual values than the linear model. This makes the quadratic model a powerful predictor, offering significant advantages for renewable energy systems. Its ability to deliver accurate energy production and consumption forecasts is particularly valuable for planning and managing renewable energy systems. This model enables more efficient evaluation of energy resources and better responsiveness to future energy demands.

However, the quadratic model's application is subject to certain limitations. The model requires sufficient data quantity and quality to ensure accurate results. It also relies on up-to-date datasets and periodic retraining to maintain its accuracy and performance. Addressing these limitations will ensure the model remains effective in evolving operational conditions.

The findings contribute to understanding and designing high-gain, dual-stage DC-DC amplifier circuits for PV power systems. Optimizing circuit parameters to achieve stable and reliable DC link voltages is crucial for integrating renewable energy sources into the grid. As demonstrated, optimizing voltage gain in cascaded DC-DC booster circuits enhances the efficiency of renewable energy systems, facilitating more effective energy conversion and utilization. Using advanced optimization techniques such as IGWO, renewable energy systems can achieve higher operational reliability through optimized parameter estimation, minimizing performance variations and uncertainties.

As a future study, an adaptive output voltage controller can be designed. With the developed IGWO algorithm, the output voltage value can be kept at 400 V levels when the converter input voltage fluctuates in the range of 40-120 V. In microgrid structures, there are high-gain converter requirements for the integration of electrical energy provided from mixed renewable energy sources into the grid/load. In this context, high-gain DC-DC converter circuits can be designed in isolated/non-isolated and cascade circuit structures. Thus, with the future smart grid structure, various mixed renewable energy sources such as solar energy, fuel cells, and wind have the potential to produce electrical energy from a few kW to MW levels.

However, the dual cascaded boost converter circuit discussed in this article suggests non-isolated high-gain applications with a parametric simulation approach. Such circuits may not be able to reach very high-power levels alone, but high-power levels can be reached with multiphase interleaved dual-cascaded DC-DC power converter circuits. In addition, the efficiency of non-isolated DC-DC boost converter circuits can reach very high levels such as 95% compared to their isolated versions. Because, isolated DC-DC power converter circuits provide an indirect conversion, and contain an inverter circuit, a high-frequency transformer, and a rectifier circuit established with high-speed diodes. The performance studies can be performed with the parametric data set approach of the isolated DC-DC power converter circuit as the future studies.

Also, the applicability of the quadratic model for different energy sources and regions can be examined in more detail, and improvements can be made to enhance the model's performance. Additionally, it is essential to compare the algorithm's effectiveness on different converter structures, such as direct current-to-current (DC-DC) converters, direct current-to-grid (DC-AC) converters, or direct current-integrated storage systems. Also, studies can be conducted examining the integration of the IGWO algorithm with real-time control systems. These studies can evaluate how the algorithm behaves under dynamic conditions and meets the real-time requirements of power electronics systems.

References

[1] L. Bagherzadeh, H. Shayeghi, S. Pirouzi, M. Shafie-khah, and J. P. S. Catalão, 'Coordinated flexible energy and self-healing management according to the multi-agent system-based restoration scheme in active distribution network', *IET Renewable Power Gen*, vol. 15, no. 8, pp. 1765–1777, Jun. 2021, doi: 10.1049/rpg2.12145.

[2] Q. Xu, N. Vafamand, L. Chen, T. Dragicevic, L. Xie, and F. Blaabjerg, 'Review on Advanced Control Technologies for Bidirectional DC/DC Converters in DC Microgrids', *IEEE Journal of Emerging and Selected Topics in Power Electronics*, vol. 9, no. 2, pp. 1205–1221, 2021, doi: 10.1109/JESTPE.2020.2978064.

[3] H. Shayeghi, S. Pourjafar, S. M. Hashemzadeh, and F. Sedaghati, 'Presenting of the Magnetic Coupling-Based Transformer-Less High Step-Up DC-DC Converter for Renewable Energy Applications', *International Transactions on Electrical Energy Systems*, vol. 3141119, pp. 1–15, Mar. 2022, doi: 10.1155/2022/3141119.

[4] M. Zadehbagheri, M. J. Kiani, S. Pirouzi, M. Movahedpour, and S. Mohammadi, 'The impact of sustainable energy technologies and demand response programs on the hub's planning by the practical consideration of tidal turbines as a novel option', *Energy Reports*, vol. 9, pp. 5473–5490, 2023.

[5] L. I. Xinze, 'Applications of Artificial Intelligence in the Circuit and Modulation Design of DC-DC Converters', 2022.

[6] S. Pirouzi, M. Zadehbagheri, and S. Behzadpoor, 'Optimal placement of distributed generation and distributed automation in the distribution grid based on operation, reliability, and economic objective of distribution system operator', *Electr Eng*, vol. 106, no. 6, pp. 7899–7912, Dec. 2024, doi: 10.1007/s00202-024-02458-w.

[7] S. Vemparala Rao and K. Sundaramoorthy, 'Performance Analysis of Voltage Multiplier Coupled Cascaded Boost Converter With Solar PV Integration for DC Microgrid Application', *IEEE Transactions on Industry Applications*, vol. 59, no. 1, pp. 1013–1023, 2023, doi: 10.1109/TIA.2022.3209616.

[8] M. Yesilbudak and M. Colak, 'Efficient parameter estimation of double diode-based PV cell model using marine predators algorithm', in *2021 10th International Conference on Renewable Energy Research and Application (ICRERA)*, IEEE, 2021, pp. 376–380. Accessed: Dec. 26, 2024. [Online]. Available: https://ieeexplore.ieee.org/abstract/document/9598635/

[9] J. López Gómez, A. Ogando Martínez, F. Troncoso Pastoriza, L. Febrero Garrido, E. Granada Álvarez, and J. A. Orosa García, 'Photovoltaic power prediction using artificial neural networks and numerical weather data', *Sustainability*, vol. 12, no. 24, p. 10295, 2020.

[10] S. Sumathi and S. Krishnan, 'Artificial Intelligence for Smart Solar Power Irrigation–Comprehensive Review', *Int. J. Adv. Sci. Eng*, vol. 7, no. 3, pp. 1894–1903, 2021.

[11] A. Mellit and S. A. Kalogirou, 'Artificial intelligence techniques for photovoltaic applications: A review', *Progress in energy and combustion science*, vol. 34, no. 5, pp. 574–632, 2008.

[12] J. Aguila-Leon, C. Vargas-Salgado, C. Chiñas-Palacios, and D. Díaz-Bello, 'Energy management model for a standalone hybrid microgrid through a particle Swarm optimization and artificial neural networks approach', *Energy Conversion and Management*, vol. 267, p. 115920, 2022.

[13] M. Quercio, L. Sabino, G. M. Lozito, R. Asghar, M. Parise, and F. R. Fulginei, 'Prediction of DC/DC Boost Converter Switching Power Losses Using a Backpropagation Algorithm Neural Network', in *2024 IEEE 8th Forum on Research and Technologies for Society and Industry Innovation (RTSI)*, IEEE, 2024, pp. 449–452. Accessed: Jan. 10, 2025. [Online]. Available: https://ieeexplore.ieee.org/abstract/document/10761247/

[14] M. Norouzi, J. Aghaei, T. Niknam, M. Alipour, S. Pirouzi, and M. Lehtonen, 'Risk-averse and flexi-intelligent scheduling of microgrids based on hybrid Boltzmann machines and cascade neural network forecasting', *Applied Energy*, vol. 348, p. 121573, 2023.

[15] K. J. Goodrick, A. Butler, T. Byrd, and D. Maksimović, 'Machine learning estimators for power electronics design and optimization', in *2021 IEEE Design Methodologies Conference (DMC)*, IEEE, 2021, pp. 1–8. Accessed: Dec. 26, 2024. [Online]. Available: https://ieeexplore.ieee.org/abstract/document/9529937/

[16] U. Yilmaz and O. Turksoy, 'Artificial intelligence based active and reactive power control method for single-phase grid connected hydrogen fuel cell systems', *International Journal of Hydrogen Energy*, vol. 48, no. 21, pp. 7866–7883, 2023.
[17] C. Chiñas-Palacios, C. Vargas-Salgado, J. Aguila-Leon, and E. Hurtado-Pérez, 'A cascade hybrid PSO feed-forward neural network model of a biomass gasification plant for covering the energy demand in an AC microgrid', *Energy Conversion and Management*, vol. 232, p. 113896, 2021.
[18] T. Sutikno, R. A. Aprilianto, and H. S. Purnama, 'Application of non-isolated bidirectional DC–DC converters for renewable and sustainable energy systems: a review', *Clean Energy*, vol. 7, no. 2, pp. 293–311, 2023.
[19] R. K. Behara and A. K. Saha, 'Artificial intelligence methodologies in smart grid-integrated doubly fed induction generator design optimization and reliability assessment: A review', *Energies*, vol. 15, no. 19, p. 7164, 2022.
[20] S. Mahjoub, L. Chrifi-Alaoui, S. Drid, and N. Derbel, 'Control and implementation of an energy management strategy for a PV–wind–battery microgrid based on an intelligent prediction algorithm of energy production', *Energies*, vol. 16, no. 4, p. 1883, 2023.
[21] M. Colak and S. Balci, 'Photovoltaic System Parameter Estimation Using Marine Predators Optimization Algorithm Based on Multilayer Perceptron', *Electric Power Components and Systems*, vol. 50, no. 18, pp. 1087–1099, Nov. 2022, doi: 10.1080/15325008.2022.2146234.
[22] S. A. Celtek, S. Kul, M. K. Singla, J. Gupta, M. Safaraliev, and H. Zeinoddini-Meymand, 'Grey wolf-based heuristic methods for accurate parameter extraction to optimize the performance of PV modules', *IET Renewable Power Gen*, vol. 18, no. 14, pp. 2248–2260, Oct. 2024, doi: 10.1049/rpg2.13061.
[23] H. Zhou *et al.*, 'Model optimization of a high-power commercial PEMFC system via an improved grey wolf optimization method', *Fuel*, vol. 357, p. 129589, 2024.
[24] 'PresentationGO, "Alternating Infographic Process for PowerPoint and Google Slides'. Accessed: Dec. 21, 2024. [Online]. Available: Available at: https://www.presentationgo.com/presentation/alternating-infographic-process-powerpoint-google-slides/
[25] R. Saravanan and N. Jaya, 'Multistage Boost Converter with Modified Voltage Multiplier for Contemporary Applications', *J. Electr. Eng. Technol.*, vol. 19, no. 7, pp. 4323–4333, Sep. 2024, doi: 10.1007/s42835-024-01857-0.
[26] N. Boujelben, F. Masmoudi, M. Djemel, and N. Derbel, 'Design and comparison of quadratic boost and double cascade boost converters with boost converter', in *2017 14th International Multi-Conference on Systems, Signals and Devices, SSD 2017*, 2017. doi: 10.1109/SSD.2017.8167022.
[27] Y. R. De Novaes, I. Barbi, and A. Rufer, 'A new three-level quadratic (T-LQ) DC-DC converter suitable for fuel cell applications', *IEEJ Transactions on Industry Applications*, vol. 128, no. 4, 2008, doi: 10.1541/ieejias.128.459.
[28] S. Balci, N. Altin, H. Komurcugil, and I. Sefa, 'Performance analysis of interleaved quadratic boost converter with coupled inductor for fuel cell applications', *IECON Proceedings (Industrial Electronics Conference)*, pp. 3541–3546, Dec. 2016, doi: 10.1109/IECON.2016.7794045.
[29] Y. Choi, J. Ji, E. Lee, S. Lee, S. Yi, and J. Yi, 'Developing Optimal Reservoir Rule Curve for Hydropower Reservoir with an add-on Water Supply Function Using Improved Grey Wolf Optimizer', *Water Resour Manage*, vol. 37, no. 5, pp. 2063–2082, Mar. 2023, doi: 10.1007/s11269-023-03478-0.
[30] M. H. Nadimi-Shahraki, S. Taghian, and S. Mirjalili, 'An improved grey wolf optimizer for solving engineering problems', *Expert Systems with Applications*, vol. 166, p. 113917, Mar. 2021, doi: 10.1016/J.ESWA.2020.113917.
[31] W. Yang, Y. Zhang, X. Zhu, K. Li, and Z. Yang, 'Research on Dynamic Economic Dispatch Optimization Problem Based on Improved Grey Wolf Algorithm', *Energies*, vol. 17, no. 6, p. 1491, 2024.
[32] Y. Qiu, X. Yang, and S. Chen, 'An improved gray wolf optimization algorithm solving to functional optimization and engineering design problems', *Scientific Reports*, vol. 14, no. 1, p. 14190, 2024.
[33] X. Zhang, W. He, and Y. Zhang, 'An adaptive output feedback controller for boost converter', *Electronics*, vol. 11, no. 6, p. 905, 2022.

[34] L. V. Bellinaso, H. H. Figueira, M. F. Basquera, R. P. Vieira, H. A. Gründling, and L. Michels, 'Cascade control with adaptive voltage controller applied to photovoltaic boost converters', *IEEE Transactions on Industry Applications*, vol. 55, no. 2, pp. 1903–1912, 2018.

[35] Y. Liu, A. As'arry, M. K. Hassan, A. A. Hairuddin, and H. Mohamad, 'Review of the grey wolf optimization algorithm: variants and applications', *Neural Comput & Applic*, vol. 36, no. 6, pp. 2713–2735, Feb. 2024, doi: 10.1007/s00521-023-09202-8.